Available online at www.sciencedirect.com
ScienceDirect
Corrosion Science 50 (2008) 1376–1384
CORROSION SCIENCE
www.elsevier.com/locate/corsci

Using EIS to analyse samples of Al–Mg alloy AA5083 treated by thermal activation in cerium salt baths

M. Bethencourt *, F.J. Botana, M.J. Cano, M. Marcos, J.M. Sánchez-Amaya, L. González-Rovira

Departamento de Ciencia de los Materiales e Ingeniería Metalúrgica y Química Inorgánica, Facultad de Ciencias del Mar y Ambientales, Universidad de Cádiz, Polígono Río San Pedro s/n, Puerto Real 11510, Cádiz, Spain

Received 6 November 2007; accepted 6 December 2007
Available online 1 February 2008

Abstract

This paper describes a study undertaken of the morphological and anticorrosive characteristics of surface layers formed on the Al–Mg alloy AA5083 from solutions of Ce(III), by means of various heat treatments while immersed in baths of cerium salts. SEM/EDS studies have demonstrated the existence of a heterogeneous layer formed by a film of aluminium oxide/hydroxide on the matrix and a series of dispersed islands of cerium deposited on the cathodic intermetallics. With the object of evaluating the degree of protection provided by the layers formed and of characterising the particular contribution of the electrochemical response of the system in NaCl, the results obtained by means of EIS are presented and discussed.

Keywords: A. Aluminium; A. Rare earth elements; B. EIS; B. SEM; C. Alkaline corrosion

1. Introduction

Prior knowledge of the behaviour and mechanism of corrosion of a metal alloy in the aggressive medium to which it will be exposed is necessary for the design of an appropriate system of protection. The corrosion behaviour of the Al–Mg alloy AA5083 in aerated solutions of NaCl 0.59 M (3.5% by weight) has been studied in several papers [1–8]; it has been found that this behaviour is conditioned by the presence and surface distribution of intermetallic precipitates, of Al (Mn, Fe, Cr) composition, that act like cathodes with respect to the matrix, without the rest of the precipitates being affected [1,2]. Thus, when a sample of the alloy AA5083 is exposed to a solution of NaCl, these precipitates of Al (Mn, Fe, Cr) act as permanent cathodes over which the following reaction takes place:

$$O_2 + 2H_2O + 4e^- \Longleftrightarrow 4OH^- \quad (1)$$

The OH^- produced by this reaction increases the pH locally, giving rise to the dissolution of the film of oxide surrounding the precipitate. In consequence, the zone of the matrix around the precipitates is left unprotected, and undergoes a process of localised alkaline corrosion (LAC). Simultaneously, a second process takes place comprising the formation on the metal matrix of a protective layer of oxide whose thickness increases with the time of exposure [1].

For this reason, the design of an effective system of protection must involve the use of cathodic inhibitors. The results of earlier studies have demonstrated that the Ce^{3+} ion is effective as a cathodic inhibitor for this alloy [5,9–11]. These results have been taken as the point of departure for the design of systems of protection based on the employment of lanthanide salts [12–15]. Studies have been made of the protective effect against corrosion in NaCl provided by treatments involving the immersion of AA5083 in solutions of salts of Ce(III) [16–19]. In accordance with the results obtained in these studies, the mechanism of protection consists of two stages. Firstly, an oxide or hydroxide

* Corresponding author. Tel.: +34 956016924; fax: +34 956016154.
E-mail address: manuel.bethencourt@uca.es (M. Bethencourt).

0010-938X/$ - see front matter © 2008 Elsevier Ltd. All rights reserved.
doi:10.1016/j.corsci.2007.12.009

of the lanthanide element is formed as a consequence of the reaction of the Ce^{3+} cation with the OH^- ions derived from the cathodic reaction taking place on the cathodic precipitates of Al (Mn, Fe, Cr). The lanthanide compound formed is highly insoluble [19,20].

In a second stage, this compound precipitates over the intermetallic particles, blocking the cathodic reaction. Consequently, the associated anodic reaction is also slowed down, resulting in times longer than 24 h being required to obtain acceptable levels of protection. These times are too long to make the application of these systems of protection viable on an industrial scale. One of the alternative means for shortening treatment times is thermal activation. In this study an accelerated method of immersion is proposed, based on increasing the temperature of the system to 363 K, which enables the optimum time of treatment to be reduced to only a few minutes.

2. Materials and experimental procedure

To carry out this study, samples of the alloy AA5083 measuring 30 × 25 × 4 mm were employed. The composition of this alloy, in percentage by mass, is shown in Table 1. Before being treated, the samples were polished on SiC paper to a finish of 500 grits. Next the samples were degreased with ethanol and cleaned carefully with distilled water.

For the immersion treatments, aerated aqueous solutions of $Ce(NO_3)_3$ and $CeCl_3$ 0.005 M were employed. One of the initial methods employed for developing protective layers consisted of the simple immersion of the aluminium alloy samples in aqueous solutions of Ce^{3+} at room temperature for exposure periods of up to 5 days.

By designing treatments involving raising the temperature of the solution during the immersion, the aluminium oxide film can be encouraged to grow over the rest of the alloy matrix, giving higher levels of protection than immersion treatments at room temperature. This process for developing layers consisted of immersing samples in solutions of Ce^{3+} at temperatures ranging from ambiental (298 K) to almost boiling point (363 K). The samples of the alloy were immersed in these solutions for periods of exposure that varied from 5 to 120 min; the temperature selected was maintained by means of a thermostatic bath (Precisterm S-138 model, from P-Selecta).

The surface appearance of the layers deposited was studied by scanning electron microscopy (SEM) using an FEG field emission microscope (Sirion model, from Phillips). Their composition was analysed by means of X-ray energy dispersive spectroscopy (XEDS) using an EDAX spectrometer, Phoenix model, connected to the cited microscope.

Table 1
Nominal composition of the alloy AA5083 (% by weight)

Mg	Mn	Si	Fe	Ti	Cu	Cr	Al
4.9	0.5	0.13	0.3	0.03	0.08	0.13	Rest

The resistance to corrosion of the samples treated can be evaluated by means of continuous current electrochemical techniques such as open circuit (OC), linear polarisations (LP) and polarisation resistance (R_p) [12]. But the information that we obtain using these techniques is only averaged. For the discriminated evaluation of the protective layer by means of continuous current, in [12] the use of the parameter passive layer resistance (R_{cp}), which corresponds to the slope on a linear scale of the passive section of the anodic branch of the LP, is proposed. Although this is also an average term, it gives us information on the resistance of the layer to polarisation.

On the other hand, for the discriminated evaluation of the different sub-processes which contribute to the overall process of corrosion can be used alternating current techniques, such as electrochemical impedance spectroscopy (EIS) [21]. In the present work, the EIS technique is employed for the evaluation and characterisation of the mixed layer formed on the samples of AA5083 in an aerated solution of NaCl 0.59 M. These measurements were conducted in a K235 flat cell, from Parc EG&G, making use of a Solartron model 1287 potentiostat coupled to a frequency response analyser (FRA), model IF 1255 from Solartron. The zone of the impedance spectrum studied corresponds to that in which the responses associated with the intermetallic precipitates and the passive film can be identified. It has been established that this range lies between 10 kHz and 1 Hz [2]. An Ag/AgCl electrode of Crison (0.207 mV/SHE) was utilised as the reference.

3. Results and discussion

As stated in the first part, the method followed for the development of protective layers consisted of immersion treatments in aqueous solutions of $Ce(NO_3)_3$ or $CeCl_3$ 0.005 M at temperatures of up to 363 K, for exposure times ranging between 0 and 120 min. Fig. 1a is a SEM image corresponding to a sample treated in $Ce(NO_3)_3$ at 363 K for 5 min; Fig. 1b shows a cross-section of an island of cerium; and Fig. 1c illustrates the appearance of the metal matrix of this sample.

The analysis of the EDS spectra confirms that the cerium is precipitated in the form of islands, Fig. 1d, preferentially on the intermetallics of Al (Mn, Fe, Cr), Fig. 1e, while the metal matrix remains free of cerium, Fig. 1f. Thus, it can be concluded that the result of these treatments is the formation of a mixed layer that consists of islands of cerium, situated over the cathodic precipitates of the alloy, and a layer of aluminium oxide/hydroxide covering the metal matrix.

With the objective of analysing the contribution of each of the interphases present in the system individually, EIS measurements of the samples treated in cerium have been made in a 0.59 M solution of NaCl. In a previous study [12] it has been demonstrated that the electrochemical response of alloy AA5083 in a solution of NaCl can be reproduced by employing an equivalent circuit as repre-

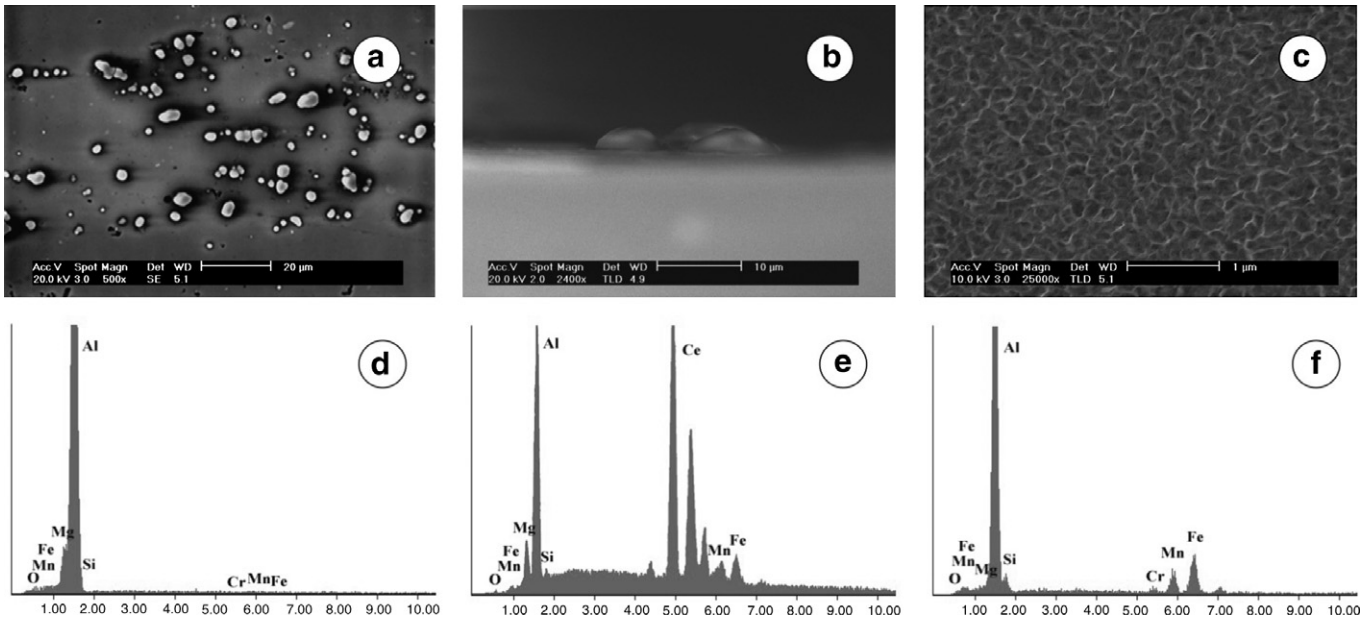

Fig. 1. (a) SEM image corresponding to a sample treated for 5 min in immersion in $Ce(NO_3)_3$ at 363 K. (b) Cross-section of an island of cerium. (c) Appearance of the metal matrix. (d–f) EDS spectra acquired, respectively, over (d) an island of cerium. (e) An Al (Mn, Fe, Cr) intermetallic. (f) The metal matrix.

sented in Fig. 2a. In this circuit, R_e is the resistance of the electrolyte, R_{int}–C_{int} is the loop associated with the reactions that take place around the intermetallics, R_{ca}–C_{ca} represents the response of the layer, R_T is the loading transfer resistance, and C_{dl} is the capacity of the double layer. This last loop gives information on the slowest processes that take place in the system, such as the transport of the Al^{+3} ions.

On the other hand, according to [12], in the presence of cerium the process of localised alkaline corrosion is slowed down. Thus the response corresponding to the intermetallics is minimised, and the R_{int}–C_{int} loop disappears. In this case, the electrochemical response of the system can be modelled by the equivalent circuit represented in Fig. 2b. This circuit can be used to simulate the electrochemical response in a solution of NaCl of the samples treated by immersion in the Ce(III) salt solution. In this circuit, the R_c–C_c loop would represent the response of the mixed layer formed on the alloy during the treatment.

The relationship between the circuits of Fig. 2a and b is given by the expressions:

$$C_c = C_{int} + C_{ca} \quad (2)$$

$$R_c = R_{int} + R_{ca} \quad (3)$$

In accordance with [12] for the case of the untreated samples, it is recommended that the circuit shown in Fig. 2a should be used, since this would provide information separately on the reactions taking place around the precipitates. Even so, the average information provided by the simulation of the response of this unprotected system using the circuit shown in Fig. 2b is also interesting. Included in Fig. 3 are the Nyquist and Bode diagrams corresponding to a sample of the alloy AA5083 immersed in NaCl. This figure also includes the simulated spectra from the fit of the experimental data to the two circuits proposed, Fig. 2a and b. The similarity existing in the fits made by applying the two circuits can be observed.

In accordance with [2] the response in impedances of the intermetallics and the layer is demonstrated in the zones of the spectrum corresponding to the high frequencies. For this reason, in order to perform the electrochemical charac-

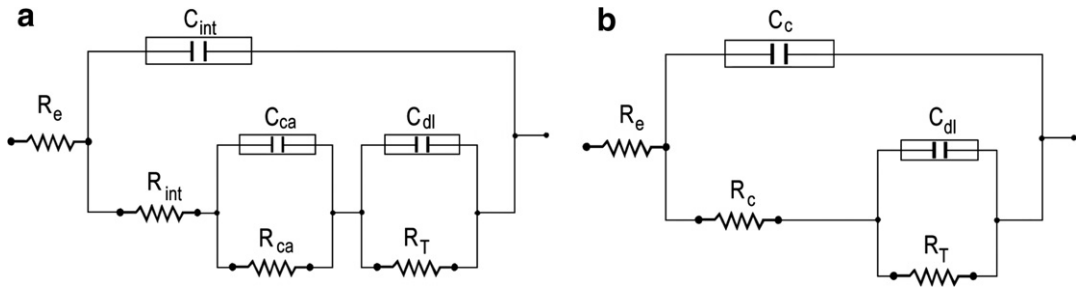

Fig. 2. Equivalent circuits proposed for simulating the electrochemical response in NaCl for (a) untreated samples, and (b) treated samples [12].

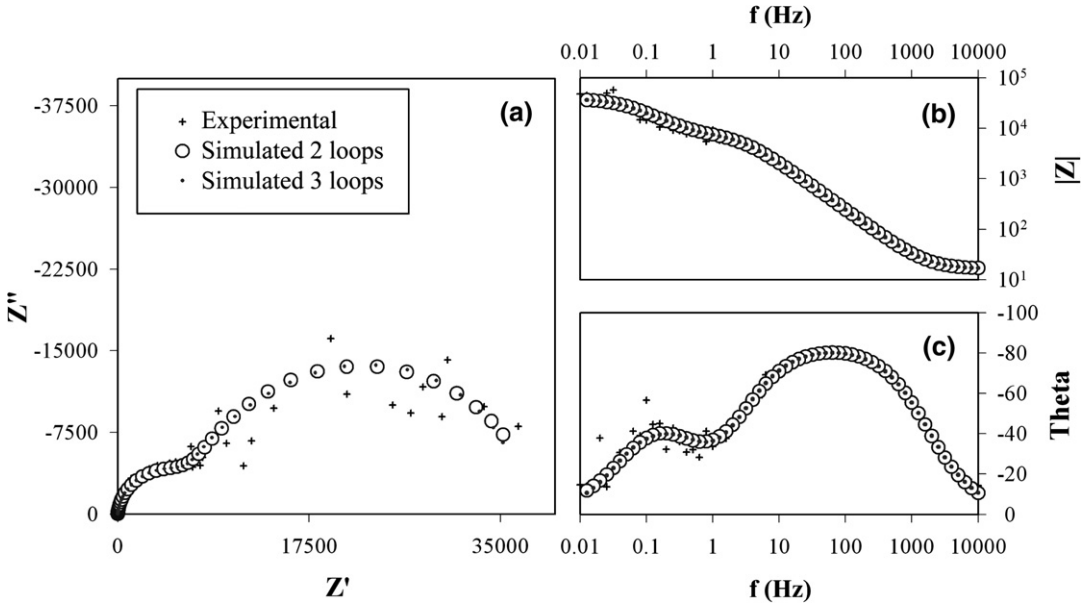

Fig. 3. EIS diagram for a sample of AA5083 in NaCl and simulation with the equivalent circuits proposed in Fig. 2a and b. Nyquist diagram (a), Bode diagram for $|Z|$ (b), and Bode diagram for the phase (c).

terisation of the mixed layer, it is necessary only to analyse the zone of the spectrum between 10 kHz and 1 Hz.

The spectra recorded for all the treated samples presented a similar appearance; Figs. 4 and 5 show the characteristic EIS spectra acquired for the samples treated by thermal activation following the different procedures described in the preceding part. For reference, the spectrum corresponding to an untreated sample has been included.

As already commented, the arc that appears in the Nyquist diagram for the case of the untreated sample corresponds to the superpositioning of the responses due to the layer and the intermetallics. In the case of the protected samples, since the process associated with the intermetallics has been minimised, the range of frequencies selected will only contain the response in impedances associated with the layer. As can be appreciated in the Nyquist diagram, for each sample treated, this arc presents a larger diameter in comparison with that of the untreated sample, which implies a higher degree of protection. That is reflected in the larger values obtained for $|Z|$, shown in the Bode diagram of Figs. 4b and 5b. In turn, the greater compacity of the layer covering the alloy is reflected in the Bode diagram for the phase, Figs. 4c and 5c. As can be observed, the spectra corresponding to the treated samples present a greater flattening of the maximum in the θ–log(f) diagram.

On the other hand, on comparing the diagrams corresponding to the protected samples, it can be observed that there is a notable difference between the spectra of the

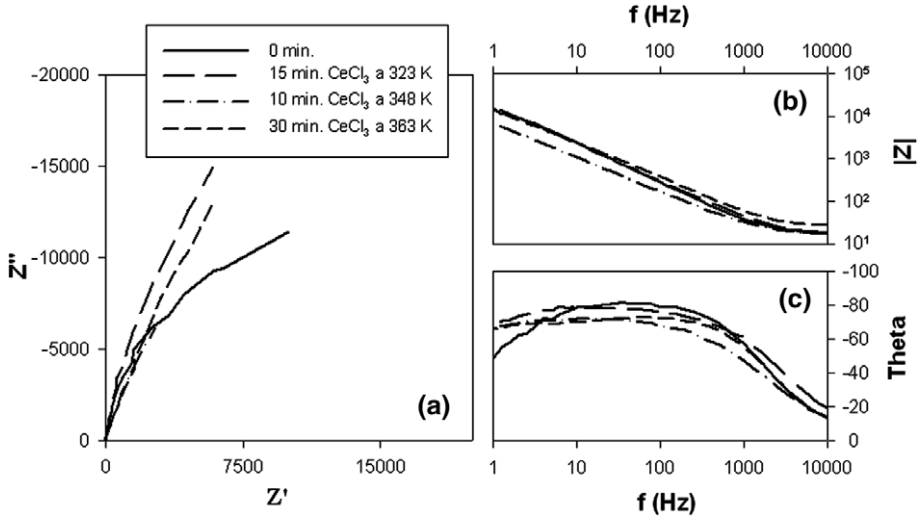

Fig. 4. Nyquist diagram (a), Bode diagram for $|Z|$ (b), and Bode diagram for the phase (c) acquired in NaCl for samples of alloy AA5083 treated by thermal activation in solution of $CeCl_3$.

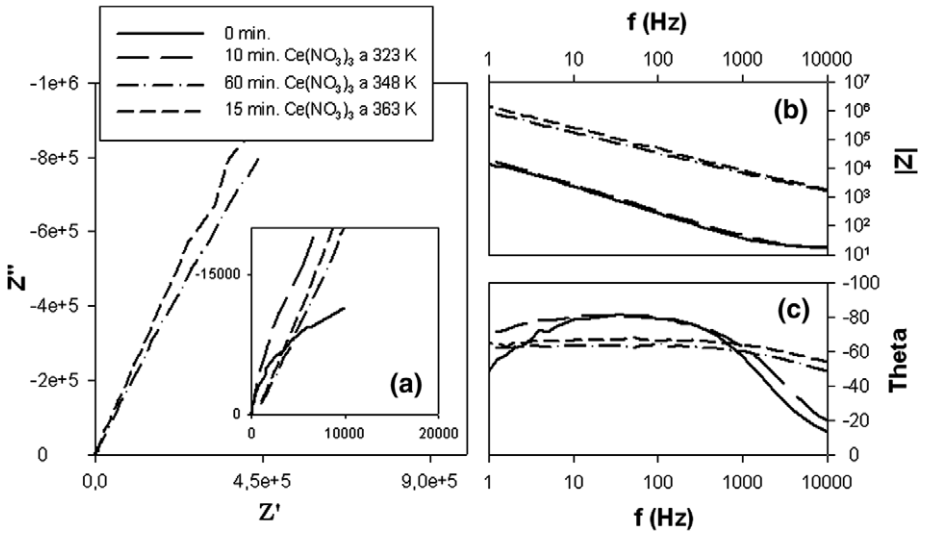

Fig. 5. Nyquist diagram (a), Bode diagram for $|Z|$ (b), and Bode diagram for the phase (c) acquired in NaCl for samples of alloy AA5083 treated by thermal activation in solution of $Ce(NO_3)_3$.

samples treated in trichloride and in cerium nitrate, which is in good agreement with the results obtained using the LP technique [22].

The points made in the preceding paragraphs should be reflected in the values of the elements that form the equivalent circuit of the system. However, in the case of the samples treated with cerium, the reactions on the intermetallics have been minimised, and so only the response associated with the mixed layer previously described has been obtained. For this reason, in order to reproduce the electrical response of the system by using equivalent circuits, it is necessary to resort to the use of the circuit shown in Fig. 2. Tables 2 and 3 give the values obtained for the elements of this circuit when fitted to the experimental data of Figs. 4 and 5. As can be seen, as the temperature is increased, the resistance of the system increases; this degree of resistance significantly exceeds the values obtained for immersion at ambient temperature, both in $CeCl_3$ and in $Ce(NO_3)_3$.

The protective effect has also evaluated in terms of the resistance of the layer. It is evident that this evaluation can be carried out in two different ways depending on whether the value of R_c, adjusted for the EIS data corresponding to the treated samples, is compared with R_{ca} or with the same R_c corresponding to the untreated sample. In the first case, according to [12], ΔR_{ca} is defined in function of R_c and R_{ca} as:

Table 2
Values of the elements of the first loop of the equivalent circuit for AA5083 in a solution of NaCl, treated by thermal activation in $CeCl_3$

T[a] (K)	t (min)	R_e (Ω cm^2)	C_c (μF cm^{-2})	φ_c	R_c (kΩ cm^2)	ΔR_{CA}	ΔR_C
Untreated	0	17.31	8.75 (C_c) 4.37 (C_{ca})	0.934	23.26 (R_c) 22.50 (R_{ca})	1	1
298	2 days	14.81	8.96	0.905	772.17	34.32	33.28
323	5	14.73	10.43	0.890	61.39	2.73	2.65
	10	13.37	12.50	0.874	91.87	4.08	3.96
	15	14.69	12.16	0.873	124.50	5.53	5.37
	30	15.41	13.46	0.891	89.86	3.99	3.87
	60	14.61	12.67	0.869	77.44	3.44	3.34
	120	14.22	15.91	0.858	95.44	4.24	4.11
348	5	16.17	14.60	0.864	90.54	4.02	3.90
	10	14.22	28.36	0.819	106.17	4.72	4.58
	15	15.33	34.04	0.805	56.96	2.53	2.46
	30	16.62	46.39	0.754	82.44	3.66	3.54
	60	24.31	69.99	0.736	151.98	6.75	6.53
	120	31.02	13.41	0.824	141.42	6.29	6.08
363	5	28.26	36.95	0.847	76.21	3.39	3.28
	10	191.0	17.15	0.857	109.33	4.86	4.71
	15	16.60	16.72	0.818	134.60	5.98	5.79
	30	21.88	11.95	0.814	137.08	6.09	5.89
	60	26.03	10.06	0.868	221.87	9.86	9.56
	120	266.30	1.62	0.658	2182.90	97.02	93.85

Table 3
Values of the elements of the first loop of the equivalent circuit for AA5083 in a solution of NaCl, treated by thermal activation in $Ce(NO_3)_3$

T^a (K)	t (min)	R_e ($\Omega\,cm^2$)	C_c ($\mu F\,cm^{-2}$)	φ_c	R_c ($k\Omega\,cm^2$)	ΔR_{ca}	ΔR_c
Untreated	0	17.31	8.75 (C_c) 4.37 (C_{ca})	0.934	23.26 (R_c) 22.50 (R_{ca})	1	1
298	2 days	15.11	8.69	0.920	267.36	11.88	11.52
323	5	15.43	9.43	0.905	91.53	4.07	3.95
	10	14.64	9.13	0.899	135.71	6.03	5.85
	15	17.73	9.14	0.919	125.68	5.59	5.42
	30	14.31	10.40	0.894	101.99	4.53	4.40
	60	14.26	12.07	0.901	125.30	5.57	5.40
	120	16.00	10.16	0.894	212.53	9.45	9.16
348	5	18.35	12.90	0.899	89.29	3.97	3.85
	10	17.16	9.12	0.902	90.32	4.01	3.89
	15	15.46	12.56	0.908	74.32	3.30	3.20
	30	28.83	12.53	0.887	73.30	3.26	3.16
	60	510.60	0.56	0.642	5770.90	256.48	248.75
	120	1623.00	0.07	0.744	6211.80	276.08	267.75
363	5	16.07	11.20	0.868	124.00	5.51	5.34
	10	29.42	9.22	0.883	182.48	8.11	7.87
	15	2452.00	0.16	0.706	32214.00	1431.73	1388.53
	30	1285.00	0.13	0.686	14085.00	626.00	607.11
	60	489.10	0.18	0.772	17066.00	758.49	735.60
	120	2587.00	0.06	0.721	428200.00	19031.11	18456.90

$$\Delta R_{ca} = \frac{R_c}{R_{ca}} \tag{4}$$

The values of ΔR_{ca} are also included in Tables 2 and 3. As can be observed, an increase in the resistance of approximately 143,000% was obtained.

It must be stated that, in this case, two different surfaces are being compared, since the presence of the precipitates in the untreated samples is being ignored. For this reason, it is interesting to analyse the improvement on average, comparing the values of R_c obtained for treated and untreated samples, according to:

$$\Delta R_c = \frac{R_c}{R_c^0} \tag{5}$$

These values have also been included in Tables 2 and 3. As can be appreciated, the highest degree of protection is provided by 15 min of treatment in $Ce(NO_3)_3$ at 363 K, which increases the average resistance by a factor of almost 140,000%.

Finally, in [12] the parameter R_{cp} was defined from the slope of the passive zone of the anodic branch. This value, determined using a stationary status technique, was justified as an average measure of the resistance of the protective layer. The validity, to a first approximation, of R_{cp} as a measure of this resistance was checked by comparing its evolution during time of treatment, with the evolution of the value of R_c [12]. These values are also compared in Fig. 6, where it can be seen that the two parameters present a similar evolution.

The protective effect has also been evaluated in terms of the C_c capacity. Thus, comparing the values corresponding to this term for the samples treated, with the value of C_{ca} obtained for the untreated sample, it can be seen how this latter value is, in almost all the cases, appreciably lower than the former values. Assuming the capacity represented in the expression (6), where ε_0 is the vacuum permittivity, ε is the dielectric constant in the film; S, the sample surface and d, the thickness of the film

$$C = \varepsilon_0 \varepsilon \frac{S}{d} \tag{6}$$

these values would indicate that the film formed on the matrix in the untreated samples is thicker than that corresponding to the mixed layer of the treated samples.

This hypothesis is in good agreement with the comments previously made. In effect, in the untreated samples, the intensity of the cathodic reaction is much greater; consequently, it is the intensity of the associated anodic reaction which must be responsible for the growth of the oxide film on the matrix. However, as the time and temperature of treatment are increased, this intensity decreases notably. This fact may be associated with beneficial effect of the temperature with the formation of a layer of oxide of sufficient thickness and compacity. Thus, in Fig. 1c, the texture of the layer formed on a sample of AA5083 by immersion in a bath of $Ce(NO_3)_3$ at 363 K for 5 min can be appreciated.

With the objective of providing an initial evaluation of the thicknesses of the films formed, cross-sections of the samples treated were analysed by scanning electron microscopy, following the procedure described in the experimental part. Fig. 7 presents SEM images of these cross-sections of samples of AA5083 treated in $Ce(NO_3)_3$ at 363 K for exposure times ranging from 5 to 120 min.

Fig. 8 shows the evolution of the thickness of the oxide/hydroxide layer formed, with time of treatment. The layer

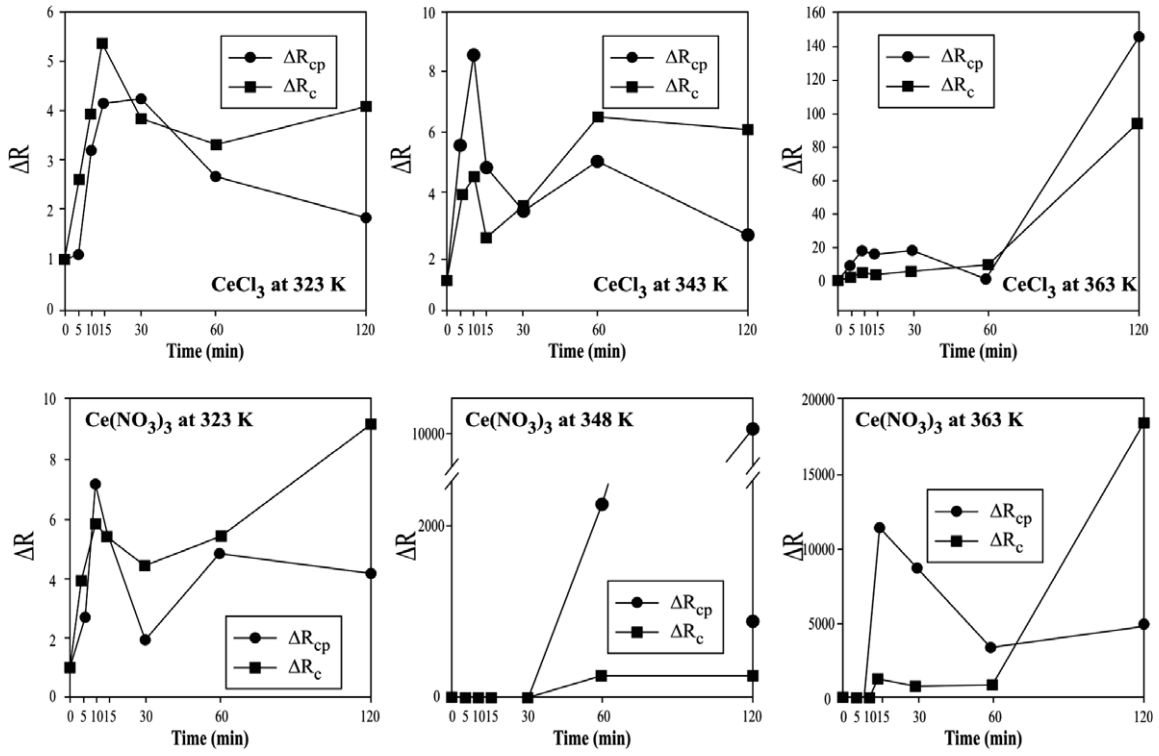

Fig. 6. Comparison of the evolutions of ΔR_{cp} and ΔR_c with time of treatment by thermal activation in solutions of $CeCl_3$ and $Ce(NO_3)_3$ at the temperatures indicated.

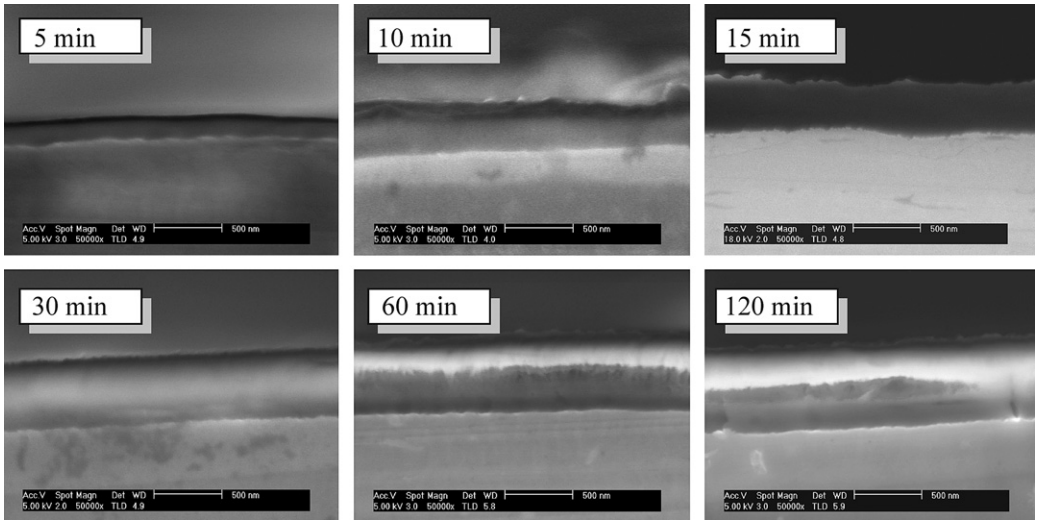

Fig. 7. SEM images of cross-sections of samples of AA5083 treated in $Ce(NO_3)_3$ at boiling point temperature for the exposure times indicated.

thickness was similarly measured for the treatments with $CeCl_3$, and the results of this are also included in Fig. 8.

One of the most notable findings is the difference in thickness obtained depending on the type of cerium salt employed. This may be due to the oxidising character of the nitrate, which would favour the formation of the layer of oxide on the metal matrix of the alloy. On the other hand, if the evolution of C_c is analysed for these cases, Fig. 8, it can be confirmed that an inverse relationship exists between the variation of the thickness and that of the capacity, which is in good agreement with the expression (6). However, this variation is not perfectly linear, Fig. 8b.

This lack of linearity may have two possible causes. One cause may be a continuous variation of the surface exposed that departs from the nominal value of 1 cm^2. However, the observations by SEM and EDS do not suggest that the value of that variation could represent such a notable deviation from linearity. In accordance with [23], the other cause of the lack of linearity between C_c and $1/d$ may be

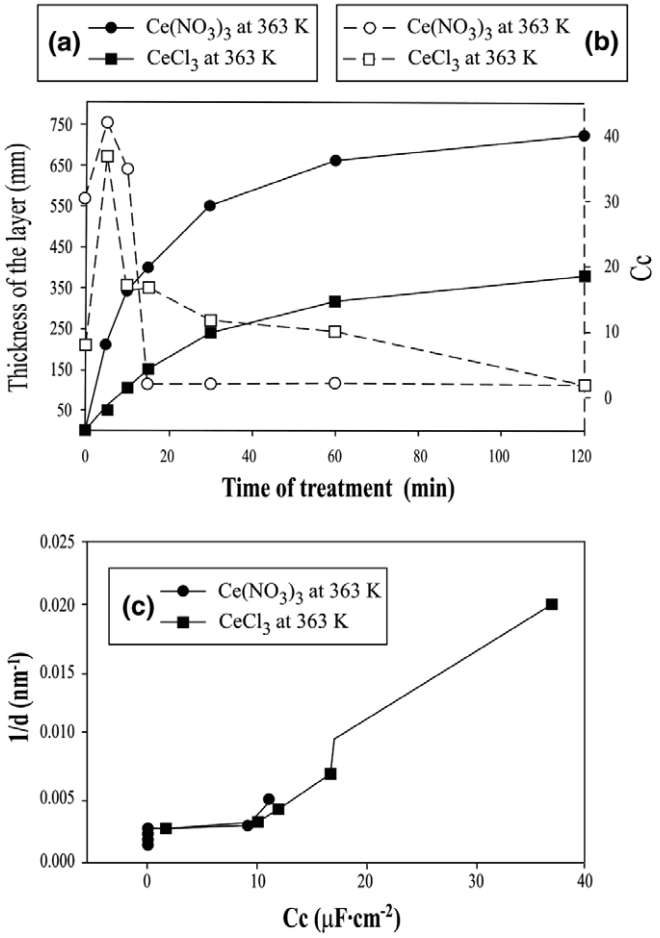

Fig. 8. (a) Evolution of the thickness of the layer and evolution of the term C_c with time of treatment in the cerium salt indicated, at boiling point temperature. (b) Relationship between the term C_c and $(1/d)$ for AA5083 in the cerium salt indicated, at 363 K.

associated with the change in the dielectric properties of the layer with time of treatment, with the consequent decrease of the value of the dielectric constant. In accordance with the preceding observations, this change would be due, basically, to the increase of its compacity.

The values of the dielectric permittivity obtained from the expression (6) are given in Table 4. It can be seen that, in each case studied, this value decreases with time of treatment, in good agreement with the previous comments.

In short, as the treatment time in solution of $Ce(NO_3)_3$, at its boiling point, is increased from 5 to 120 min, not only are the cathodic points of the alloy blocked and a layer of aluminium oxide/hydroxide is formed on the metal matrix but also, the dielectric properties of this layer are modified; this makes the layer act as a better insulating barrier, which is the factor responsible for the extremely high values obtained for the different resistances by the various techniques employed.

Comparing these values obtained for the treatments in $Ce(NO_3)_3$ and $CeCl_3$, a considerable difference can be observed, since the thicknesses obtained with nitrate are not obtained with the cerium chloride salt, nor is the quality of the protective layer comparable. This indicates that the anion selected for these treatments plays a very important role in the development of systems of protection, especially in respect of the formation of the oxide film on the matrix.

4. Conclusions

Immersion treatments of the Al–Mg alloy AA5083 in solutions of Ce(III) salts lead to the formation of a mixed layer consisting of island of cerium situated over the cathodic intermetallic compounds present on the surface, and a film of alumina that covers the rest of the metal matrix. When these treatments are applied at room temperature, the optimum time of treatment is conditioned by the slow rate at which the oxide film over the matrix is produced, and requires two days of treatment to obtain acceptable degrees of protection.

In order to accelerate the formation of the protective layer, immersion treatments in solutions of $Ce(NO_3)_3$ and $CeCl_3$ at 363 K have been conduced. SEM and EDS studies reveal that a heterogeneous layer is formed onto the surface of the alloy. This layer is composed by cerium-rich dispersed islands placed onto the cathodic particles and an alumina film covering the metallic matrix.

It is significant that the treatment times required to obtain excellent levels of protection do not exceed 15 min, which should make the treatments attractive to industry.

Electrochemical impedance spectroscopy (EIS) has been applied to evaluate the influence of the Ce(III) salts on the electrochemical response of the sub-processes that take place when the alloy AA5083 is corroding in NaCl solution. Using EIS, it was possible to detect the blocking of the cathodic sites. The inhibition effect is reflected in the

Table 4
Values of the parameters related to the protective layer formed in salt of cerium(III), at boiling point temperature and for the times indicated

Time	$Ce(NO_3)_3$			$CeCl_3$		
	C_c (10^{-6} F)	Thickness (10^{-6} cm)	ε calculate	C_c (10^{-6} F)	Thickness (10^{-6} cm)	ε calculate
5	11.20	211	266.69	36.95	50	208.66
10	9.22	344	357.75	17.15	105	203.38
15	0.16	398	7.18	16.72	150	283.26
30	0.13	549	8.06	11.95	243	327.96
60	0.18	659	13.40	10.06	316	359.03
20	0.06	720	4.88	1.62	408	74.64

electrical response of the system by the minimisation of the values of those elements of the electrical loop related to the response of the cathodic intermetallics. The results suggest that the layer developed protects the alloy against the localised alkaline corrosion (LAC) process, which is the main corrosion process that takes place on the alloy when it is exposed to NaCl solutions, in the same way that those previously obtained by full immersion treatments carried out at room temperature.

References

[1] A. Aballe, M. Bethencourt, F.J. Botana, M.J. Cano, M. Marcos, Localized alkaline corrosion of alloy AA5083 in neutral 3.5% NaCl solutions, Corros. Sci. 43 (2001) 1657–1674.

[2] A. Aballe, M. Bethencourt, F.J. Botana, M.J. Cano, M. Marcos, Inhibition of the corrosion process of alloy AA5083 (Al–Mg) in seawater by cerium cations. An EIS study, Mater. Corros. 52 (2001) 344–350.

[3] A. Aballe, M. Bethencourt, F.J. Botana, M. Marcos, J. Pérez, M.A. Rodríguez-Chacón, Electrochemical impedance spectroscopy study of the behavior of lanthanide-rich films formed on Al–Mg alloys, Mater. Sci. Forum 289–292 (1998) 557–566.

[4] A. Aballe, M. Bethencourt, F.J. Botana, J. Pérez, M. Marcos, M.A. Rodríguez, Estudio mediante EIS de la respuesta electroquímica de la aleación AA5083 frente a señales DC anódicas, Rev. Metal. Madrid 34 (1998) 37–41.

[5] M. Bethencourt, F.J. Botana, M.A. Cauqui, M. Marcos, M.A. Rodríguez, J.M. Rodríguez Izquierdo, Protection against corrosion in marine environments of AA5083 Al–Mg alloy by lanthanide chlorides, J. Alloy Compd. 250 (1997) 455–460.

[6] M.A. Arenas, M. Bethencourt, F.J. Botana, J.J. Damborenea, M. Marcos, Inhibition of AA5083 aluminium alloy and galvanised steel by lanthanide salts, Corros. Sci. 43 (2001) 157–170.

[7] A. Aballe, M. Bethencourt, M.J. Cano, M. Marcos, EIS study of the electrochemical response of AA5083 alloy under anodic polarisation, Corros. Rev. 18 (1) (2000) 1–11.

[8] A. Aballe, M. Bethencourt, F.J. Botana, M.J. Cano, M. Marcos, On the reproducibility of the electrochemical response of AA5083 alloy in NaCl solutions, in: B.A. Shaw, R.G. Buchheit, J.P. Moran (Eds.), Corrosion and Corrosion Prevention of Low Density Metals and Alloys, The Electrochemical Society Inc., Pennington, 2001, pp. 364–375.

[9] A. Aballe, M. Bethencourt, F.J. Botana, M. Marcos, $CeCl_3$ and $LaCl_3$ binary solutions as environmentally friendly corrosion inhibitors of AA5083 aluminum alloy in NaCl solutions, J. Alloy Compd. 323–324 (2001) 855–858.

[10] A.K. Mishra, R. Balasubramaniam, Corrosion inhibition of aluminium alloy AA 2014 by rare earth chlorides, Corros. Sci. 49 (2007) 1027–1044.

[11] A.K. Mishra, R. Balasubramaniam, Corrosion inhibition of aluminium alloy 6061 by rare earth chlorides, Corrosion 63 (3) (2007) 240–248.

[12] A. Aballe, M. Bethencourt, F.J. Botana, M.J. Cano, M. Marcos, On the mixed nature of cerium conversion coatings, Mater. Corros. 53 (2002) 176–184.

[13] A. Aballe, M. Bethencourt, F.J. Botana, M. Marcos, J.M. Sánchez-Amaya, Alternativas al cromo en la industria del acabado superficial del aluminio. Tratamientos superficiales de bajo impacto medioambiental, Rev. Metal. Madrid 37 (2001) 49–62.

[14] M.A. Arenas, R. Rodríguez, J.J. Damborenea, Effect of cerium and lanthanum ion implantation on corrosion behaviour of hot dip galvanized steel, Rev. Metal. Madrid 37 (5) (2001) 591–596.

[15] A.M. Cabral, W. Trabelsi, R. Serra, M.F. Montemor, M.L. Zheludkevich, M.G.S. Ferreira, The corrosion resistance of hot dip galvanised steel and AA2024-T3 pre-treated with bis-[triethoxysilylpropyl] tetrasulfide solutions doped with $Ce(NO_3)_3$, Corros. Sci. 48 (2006) 3740–3758.

[16] A.J. Aldykewicz, H.S. Isaacs, A.J. Davenport, The investigation of cerium as a cathodic inhibitor for aluminium–copper alloys, J. Electrochem. Soc. 142 (10) (1995) 3342–3350.

[17] Y.C. Lu, M.B. Ives, Chemical treatment with cerium to improve the crevice corrosion resistance of austenitic stainless steels, Corros. Sci. 37 (1) (1995) 145–155.

[18] M. Dabala, L. Armelao, A. Buchberger, I. Calliari, Cerium-based conversion layers on aluminium alloys, Appl. Surf. Sci. 172 (3–4) (2001) 312–322.

[19] K. Aramaki, Treatment of zinc surface with cerium(III) nitrate to prevent zinc corrosion in aerated 0.5 M NaCl, Corros. Sci. 43 (11) (2001) 2201–2215.

[20] M. Bethencourt, F.J. Botana, M.J. Cano, M. Marcos, High protective environmental friendly and short-time developed conversion coatings for aluminium alloys, Appl. Surf. Sci. 189 (2002) 162–173.

[21] R.J. Scully, Electrochemical methods in corrosion testing, in: J.R. Davis (Ed.), Handbook, ninth ed., vol. 13, American Society for Metals Handbook, Metals Park, OH, 1987, pp. 212–220.

[22] M. Bethencourt, F.J. Botana, M.J. Cano, M. Marcos, R.M. Osuna, Combination of thermal activation and addition of H_2O_2 to improve cerium based immersion treatment of alloy AA5083, Mater. Corros. 54 (2003) 77–83.

[23] M. Marcos, Introduction to Electrostatic, third ed., University de Cadiz, Cadiz, 1995.